

THE RELATION BETWEEN MAGNETIC FIELDS AND CORONAL ACTIVITIES IN THE POLAR CORONAL HOLE

MASUMI SHIMOJO¹ AND SAKU TSUNETA²

¹ Nobeyama Solar Radio Observatory, Nobeyama, Nagano, 384-1305, Japan; shimojo@nro.nao.ac.jp

² National Astronomical Observatory of Japan, Mitaka, Tokyo, 181-8588, Japan
Received 2009 July 2; accepted 2009 October 19; published 2009 November 4

ABSTRACT

We investigated the relation between polar magnetic fields and polar coronal activities based on Stokes maps of photospheric and chromospheric lines, simultaneous X-ray and EUV images. These images are taken with *Hinode* and *Solar and Heliospheric Observatory*. With careful co-alignment between these images, we found that the X-ray jets, the X-ray bright points, and the coronal loops in the polar coronal hole appear around the relatively large magnetic concentrations near the kG-patches with minority polarity. The magnetic concentrations have magnetic polarity opposite to that of kG-patches, and they are clearly identified in the Stokes-*V* maps of the Na I line. We also found that such minority magnetic concentrations emerge from below the photosphere in the polar region. Our results suggest that the coronal activities and structures in the polar coronal hole can be used as a tracer of the appearance of the minority polarities in the polar region.

Key words: Sun: corona – Sun: magnetic fields – Sun: X-rays, gamma rays

Online-only material: animation

1. INTRODUCTION

One of the new discoveries obtained by *Hinode* (Kosugi et al. 2007) is the activity in the polar region of the Sun. Using high-cadence X-ray images taken by the X-Ray Telescope (XRT; Golub et al. 2007; Kano et al. 2007) aboard *Hinode*, Savcheva et al. (2007) found that polar X-ray jets around the south pole occur at very high frequency, about 60 jets per day on average. Cirtain et al. (2007) revealed that polar X-ray jets have two components and that the velocity of the faster component is close to the local Alfvén speed. They suggest that the Alfvén wave is generated by the jets. It is possible that the Alfvén waves generated by numerous X-ray jets contribute to the acceleration of the fast solar wind.

Another new result obtained by *Hinode* is concerned with the magnetic field measurement of the solar polar region with high polarimetric accuracy. With the Solar Optical Telescope (SOT; Tsuneta et al. 2008a; Suematsu et al. 2008; Ichimoto et al. 2008; Shimizu et al. 2008) aboard *Hinode*, Tsuneta et al. (2008b) found that many vertically oriented magnetic flux tubes with field strength as strong as 1 ~ 1.2 kG are scattered in latitude between 70° and 90° and all the fluxes have the same sign consistent with the global polar field. If the flux tubes extend to the interplanetary space, there will be a possibility that they serve as the guide fields for X-ray jets, coronal plumes, and the fast solar wind. In this Letter, we present the results of accurate co-alignment between Stokes maps of photospheric and chromospheric lines, and X-ray and EUV images. With these co-aligned maps, we describe the relation between the magnetic fields at the lower atmosphere and the coronal activities in the polar coronal hole.

2. THE OBSERVATIONS

In 2007 September, *Hinode* observed the north pole for a month. We here used a part of the data set obtained during the period. The Filtergraph of the SOT (SOT-FG) obtained the following data during the period: the *G*-band 4305 Å, the Ca II

H 3968 Å, and the Stokes-*I, V* components of the Na I 5896 Å. The Stokes-*V* signal of the Na I line indicates the line-of-sight component of magnetic fields in the lower chromosphere or the upper photosphere. The time cadence of the images is 4 minutes. In this Letter, *G*-band and Ca II H images are used for the co-alignment purpose. The field of view was 276'' × 163'' with a pixel size of 0'.160 for the Na I images. The Stokes-Polarimeter of the SOT (SOT-SP) obtained the full Stokes profiles of two Fe I lines at 6301.5 Å and 6302.5 Å with a wavelength sampling of 21.6 Å. The scanning field of view was 268'' × 162'' with a pixel size 0'.147 × 0'.158. It took about 5 hr for scanning the field of view. The XRT obtained the X-ray images using the thin Al-poly filter during the period. The analysis filter provides the sensitivity above 2 MK. The time cadence was 2 minutes. The field of view was 1053'' × 394'' with a pixel size 1'.028. The XRT also took *G*-band full-Sun images when it started a new observing sequence. In order to identify cooler coronal structures, we also used the EUV images taken by the Extreme ultraviolet Imaging Telescope (EIT; Delaboudinière et al. 1995) aboard *Solar and Heliospheric Observatory* (*SOHO*; Domingo et al. 1995).

3. CO-ALIGNMENT BETWEEN THE SOT, THE XRT, AND THE EIT

The pointing offset between the XRT and the SOT consists of the stable component and the time-varying component because the pointing of each telescope changes due to the thermal drift of the telescopes and due to the image stabilization system of the SOT. We performed co-alignment based on the methodology proposed by Shimizu et al. (2007). We describe the details of the method as applied to our data set.

In the first step, we co-aligned the time series of the images obtained by each telescope. In the case of the XRT, the main component of the pointing drift is due to the jitter motion of the satellite and the thermal drift with the orbital phase. In order to correct the drift, we used the IDL program "xrt_jitter.pro" (Shimizu et al. 2007) in the Solar SoftWare (SSW; Freeland &

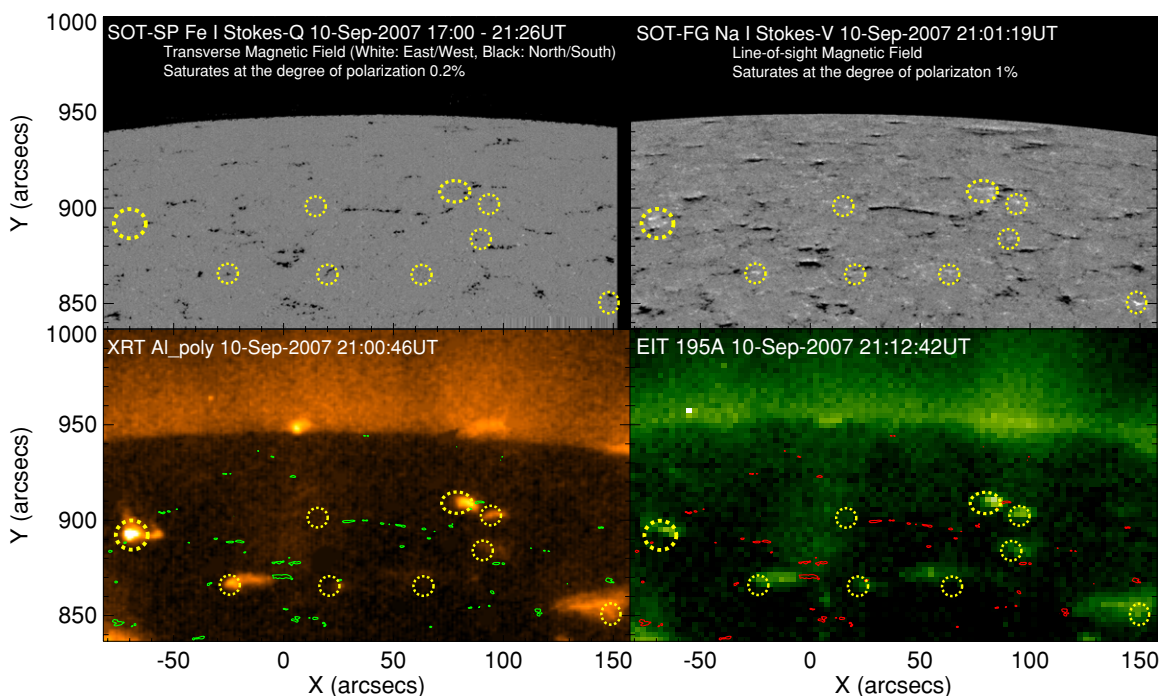


Figure 1. North pole images around 21:00 UT on 2007 September 10. The yellow dash circles indicate the relatively large minority poles identified in the Na I Stokes-V map. The green and the red lines in the lower panels are the contours of the degree of polarization (1%) of the Fe I Stokes-Q map.

Handy 1998). The alignment accuracy of the XRT images is less than $1''$.

The pointing drift of the SOT is corrected by the onboard image stabilization system (Shimizu et al. 2008) that detects the pointing drift from the pattern of the granules. During the polar observations, the granule images taken for the image stabilization become fuzzy by the foreshortening effect. As a result, the pointing of the SOT gradually drifts to one direction. If the duration of an observation is longer than a few tens of minutes, the drift becomes prominent in the images. In this Letter, we co-aligned the time series of the SOT images using the cross correlation technique and the solar limb as a fiducial mark. The alignment accuracy of the SOT images is within a few arcseconds during the observation period. The filter-dependent pointing offsets were collected based on Shimizu et al. (2007).

We co-aligned the XRT images and the SOT images based on the DC-pointing offset derived by Shimizu et al. (2007). For the co-alignment, we have to consider the effect of the image stabilization system of the SOT. The DC-pointing offset is valid only when the tip-tilt mirror sits at the null point. In order to remove the hysteresis of the null point associated with the Piezo actuator, the image stabilization system is reset and restarted before starting the new SOT observing sequence. Hence, the first G-band image taken by the SOT can be co-aligned with the first G-band image taken by the XRT based on the known DC-pointing offset. After performing the co-alignment between the G-band SOT/XRT images based on the DC-pointing offset, we performed a minor adjustment and confirmed the co-alignment using the solar limb as the fiducial mark. The co-alignment accuracy between the first G-band images taken by the SOT and the corresponding XRT image is less than a pixel size of the XRT.

Because we already co-aligned the time series of the images obtained by each telescope, the whole time series of the Na I images taken with the SOT-FG and the XRT images are co-aligned by applying the offset derived by the initial pair of

G-band XRT/SOT images. It is difficult to verify the accuracy of the co-alignment over the observing period because there is no structure as a fiducial mark except the solar limb. The accuracy of our co-alignment is roughly less than a few arcseconds based on the difference between the limbs of the Na I and the X-ray images. We point out that this accuracy is enough to discuss the relation between coronal activities and magnetic fields.

In order to co-align the SOT-SP data with other images, we can use the Stokes-V features obtained by the SOT-SP and the SOT-FG. However, the co-alignment accuracy between the Stokes maps obtained by the SOT-SP and the Na I Stokes-V images taken by the SOT-FG is larger than $5''$ in the worst case, simply because the magnetic features are changing during 5 hr, which is the time required to obtain a single set of the SOT-SP data in this case. For the co-alignment between the EUV images obtained by the EIT and the XRT images, we used the coronal structures as the fiducial marks.

4. CORONAL ACTIVITIES AND MAGNETIC FIELDS IN THE POLAR CORONAL HOLE

Figure 1 shows the co-aligned images taken by the SOT, the XRT, and the EIT on 2007 September 10. In the Stokes-Q map in Figure 1, the magnetic patches are easily seen in black. The average of the maximum magnetic field strength of the scattered patches is 1.5 kG. The properties of the magnetic patches were reported by Tsuneta et al. (2008b), and they called such patches the kG-patches. The Stokes-V map of the Na I line shows the bipolar structures at the locations of these kG-patches. It indicates that the patches have the fanning-out magnetic structures in the lower chromosphere or in the higher photosphere. The polarity of the patches is the same as that of the global polar field.

The contours in the lower panels in Figure 1 indicate the degree of polarization (1%) of the Fe I Stokes-Q map. The contours coincide in position with the kG-patches. Comparing

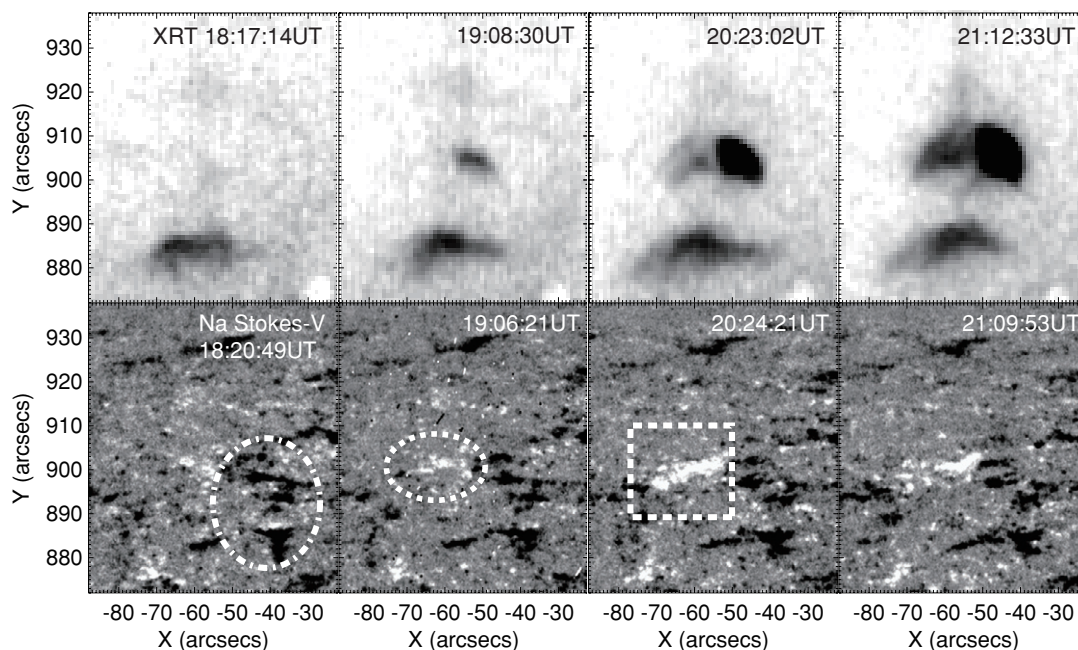


Figure 2. Example of a polar X-ray jet associated with the emerging fluxes. Upper panels: the X-ray (negative) images. Lower panels: the Na I Stokes-V maps. The dotted-dashed circle indicates the kG-patches interacted with the emerging fluxes. The dashed circle indicates the emerging flux region. The dashed box indicates the FOV of panel A in Figure 3.

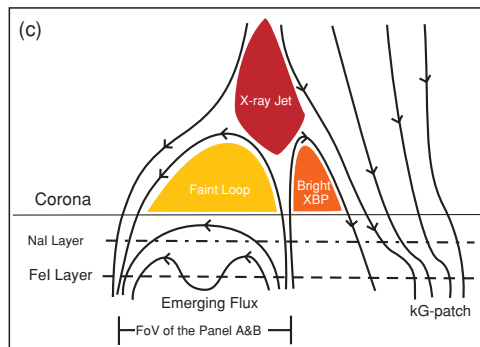
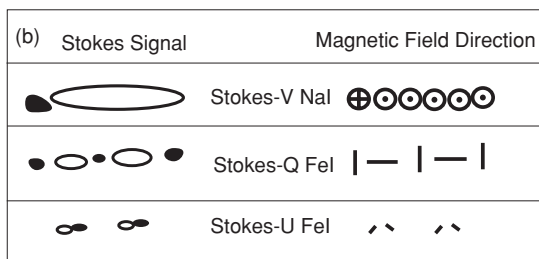
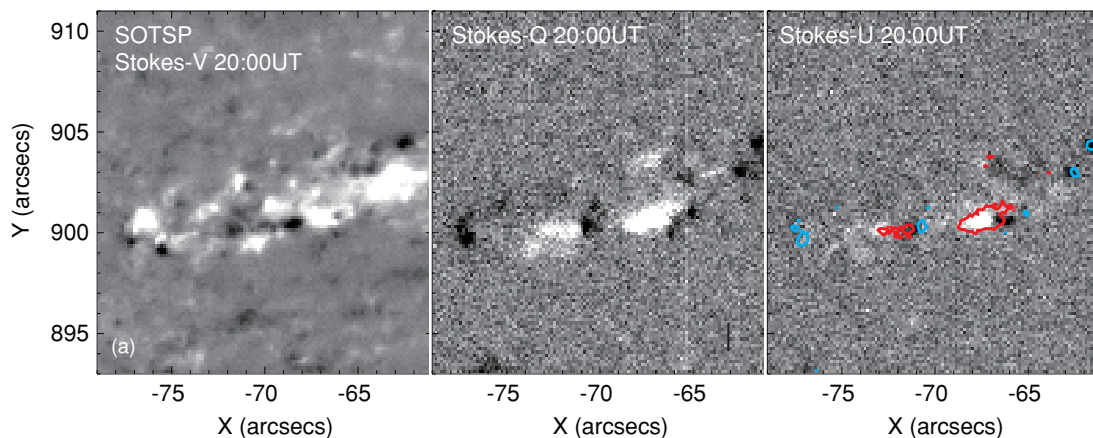


Figure 3. Magnetic fields around the polar X-ray jet. (a) The Fe I Stokes-V, Q, and U maps obtained by the SOT-SP. The red and the blue contours in the Stokes-U map indicate the degree of polarization (1%) of Stokes-Q. The red (blue) contours indicate the magnetic fields that are directed to the east (west) (north/south). (b) Left: schematic pictures of the Stokes signals of the emerging flux region. Right: the magnetic field directions based on the Stokes maps. (c) The magnetic field configuration of the jet based on the Stokes maps. Panels (a) and (b) show only the emerging flux region.

the contours with the coronal structures in the X-ray and the EUV images, we see that most of the kG-patches are not associated with the coronal structures. The movie in Figure 4 (available in the online journal) is the Na I Stokes-V movie that is overlaid by the co-aligned X-ray movie. The movie in Figure 4 also shows that there is essentially not any coronal

structures/activities on most of the kG-patches. In contrast, it appears that the X-ray bright points (XBPs), the X-ray jets, or the coronal loops are located around, not at, the positions of the kG-patches. But not all the kG-patches are associated with such coronal activities. What is the origin of the difference between the kG-patches with and without the coronal activities/

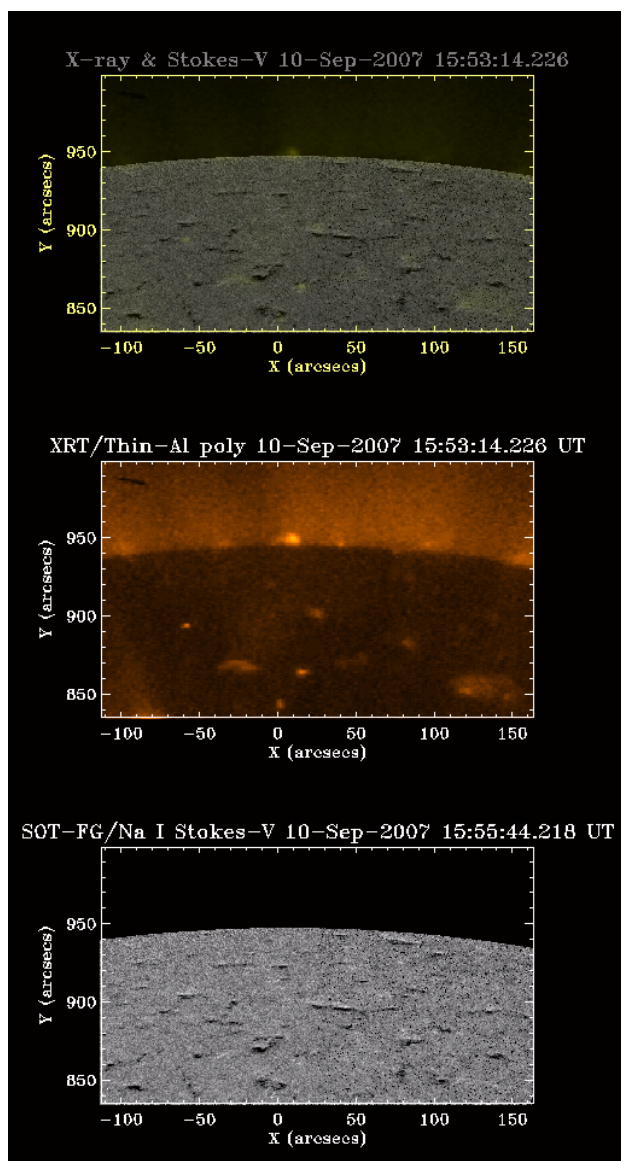


Figure 4. Coronal hole around the north pole. Upper panel: the gray scale presents the Stokes- V signals of the Na I line and the yellow indicates the X-ray intensity. Middle panel: X-ray. Lower panel: Stokes- V signals of the Na I line.

(An animation of this figure is available in the online journal.)

structures? In the Na I Stokes- V maps, there are the relatively large positive (white) patches (the yellow circles in Figure 1) under the coronal structures. It appears that the coronal loops and the XBPs bridge the negative kG-patches and the positive patches. Note that the polarity of the positive patches is opposite to the global polar field. The magnetic field strength of the positive patches is weaker than the negative kG-patches, since there is no Fe I Stokes- Q and U signal at the location of the positive patches. Consequently, we conclude that the coronal structures and activities in the polar coronal hole appear when and where the relatively large magnetic fields with minority polarity appear near the kG-patches in the lower atmosphere.

5. THE EMERGING FLUX IN THE POLAR CORONAL HOLE

In the previous section, we report that there are the relatively large magnetic concentrations with minority polarity near the kG-patches under all the coronal structures and activities in

the polar coronal hole. Where do such minority poles come from? From the movie in Figure 4, we found that some minority polarities emerge from below the photosphere followed by the appearance of the coronal structures/activities above the minority polarities. In order to confirm where the minority polarity came from, we examined a polar X-ray jet that occurred on the minority polarity that had Fe I Stokes- Q and U signals.

Figure 2 shows the polar X-ray jet that occurred on 2007 September 6. At first, in the X-ray images, an XBP appeared around 18:30 UT. The brightness and the size of the XBP rapidly increased after 19:20 UT, and the X-ray jet started around 20:00 UT. The jet disappeared around 23:00 UT. From the Na I Stokes- V maps, the black and white patches appeared around 19:00 UT, and spread out in the direction of east and west. The apparent evolution is similar to that of the emerging flux regions in the quiet Sun near the disk center.

Panel (a) of Figure 3 is the Fe I Stokes- V , Q , and U maps taken by the SOT-SP. Panel (b) shows the schematic pictures of the Stokes maps and the directions of the magnetic fields based on the Stokes signals. The directions of the magnetic fields support the magnetic field configuration described as follows. In the lower chromosphere/upper photosphere (the Na I layer), the simple Stokes- V signal distribution indicates a simple loop system (panel (c)). In the lower photosphere (the Fe I layer), the magnetic fields are not so simple. There are the Stokes- U bipolar structures in the positive signal regions of the Stokes- Q . It suggests that the magnetic fields are meandering like a sea serpent. Such structures are seen in the emerging flux region (Bernasconi et al. 2002). Based on these pieces of evidence, the increase of the positive signals in the Na I Stokes- V maps under the polar X-ray jet indicates the actual emerging flux, and it is not due to the change in the direction of the magnetic field vector.

We can easily find such increases of the positive signals that are associated with the polar X-ray jets from the movie of the Na I Stokes- V maps. The movie in Figure 4 shows that such events occurred at the approximate coordinates (90, 910) and (−70, 895). The spatial relation between the X-ray structures and the Na I Stokes- V signals of the events is the same as that of the event described in the section. Hence, we conclude that the increases of the positive signals in the Na I Stokes- V maps indicate the emerging flux regions.

6. CONCLUSION AND DISCUSSION

We obtain the spatial relation between polar magnetic fields and polar coronal activities/structures with careful co-alignment among the Stokes maps of the lower atmosphere, X-ray images and EUV images. We found that the coronal structures and activities appear when the relatively large magnetic concentrations with minority polarity appear near the kG-patches, and we also verified that the increases of the minority signals that are associated with the polar X-ray jets in the Na I Stokes- V indicate the emerging flux regions. Since the relation between the coronal structures and the magnetic concentrations with minority polarity can be easily found from other data set of the polar region, the relation is very rigid. The result suggests that the coronal structures and activities in the polar coronal hole are produced by the interactions of the kG-patches with the emerging minority polarities near the kG-patches. Kamio et al. (2009) also reported the same relation based on the EUV observations. Hence, the coronal activities and structures in the polar coronal hole can be used to detect the appearance of the minority polarity in the polar region. Recently, Savcheva et al. (2009) showed that the

direction of the magnetic field is derived from the transverse motion in an X-ray jet. Based on our and their results, we may be able to understand the polarity inversion by the continuous monitoring of the polar coronal activities.

We show that the emerging flux appears even in the polar region. It may not be conceivable that the magnetic flux located in the middle latitude of the convection zone emerges at the polar region. The emerging flux in the polar region may be generated by the local dynamo process due to the granular/super-granular motion. Recently, Ishikawa & Tsuneta (2009) showed the evidence that the local dynamo process generates weak horizontal magnetic fields. Our result also indicates that the local dynamo process works in the polar region.

Finally, we discuss the relation between the kG-patches, the X-ray jets, and the fast solar wind. The kG-patches provide all the open magnetic fields that serve as the channels of the fast solar wind (Tsuneta et al. 2008b). If the X-ray jets provide the energy for the acceleration of the fast solar wind, the X-ray jets have to occur at around almost all of the kG-patches. However, most of the kG-patches are not associated with the X-ray jets. Thus, it is unlikely that the polar X-ray jets provide sufficient energy for the acceleration of the fast solar wind. The energy may be provided by weak activities without involving coronal X-ray jets.

We started the study from the Nobeyama/*Hinode* Coordinated Data Analysis Workshop 2007 at Nobeyama Solar Radio Observatory. We thank the participants of the NSRO/*Hinode*-CDAW07. We also thank T. Shimizu, Y. Katsukawa, and S. Kamio for helpful comments and discussions. *Hinode* is a Japanese mission developed and launched by ISAS/JAXA,

collaborating with NAOJ as a domestic partner, NASA and STFC (UK) as international partners. Scientific operation of the *Hinode* mission is conducted by the *Hinode* science team organized at ISAS/JAXA. This team mainly consists of scientists from institutes in the partner countries. Support for the post-launch operation is provided by JAXA and NAOJ (Japan), STFC (U.K.), NASA, ESA, and NSC (Norway). We are grateful for the use of EIT data obtained on the *SOHO* spacecraft. *SOHO* is project of international cooperation between ESA and NASA. This work was carried out at the NAOJ *Hinode* Science Center, which is supported by the Grant-in-Aid for Creative Scientific Research “The Basic Study of Space Weather Prediction” from MEXT, Japan (Head Investigator: K. Shibata), generous donations from Sun Microsystems and NAOJ internal funding.

REFERENCES

- Bernasconi, P. N., et al. 2002, *Sol. Phys.*, 209, 119
Cirtain, J. W., et al. 2007, *Science*, 318, 1580
Delaboudinière, J.-P., et al. 1995, *Sol. Phys.*, 162, 291
Domingo, V., Fleck, B., & Poland, A. I. 1995, *Sol. Phys.*, 162, 1
Freeland, S. L., & Handy, B. N. 1998, *Sol. Phys.*, 182, 497
Golub, L., et al. 2007, *Sol. Phys.*, 243, 63
Ichimoto, K., et al. 2008, *Sol. Phys.*, 249, 233
Ishikawa, R., & Tsuneta, S. 2009, *A&A*, 495, 607
Kamio, S., et al. 2009, *A&A*, 502, 345
Kano, R., et al. 2008, *Sol. Phys.*, 249, 263
Kosugi, T., et al. 2007, *Sol. Phys.*, 243, 3
Savcheva, A., et al. 2007, *PASJ*, 59, 771
Savcheva, A., Cirtain, J. W., DeLuca, E. E., & Golub, L. 2009, *ApJ*, 702, L32
Shimizu, T., et al. 2007, *PASJ*, 59, S845
Shimizu, T., et al. 2008, *Sol. Phys.*, 249, 221
Suematsu, Y., et al. 2007, *Sol. Phys.*, 249, 197
Tsuneta, S., et al. 2008, *Sol. Phys.*, 249, 167
Tsuneta, S., et al. 2008, *ApJ*, 688, 1374